Electronic supplementary information

Homo- and hetero-dinuclear Pt(II)/Pd(II) complexes: studies of the hydrolysis, nucleophilic substitution reactions, DNA/BSA interactions, DFT calculation, molecular docking and cytotoxic activity

Dušan Ćoćić,[1] Snežana Jovanović-Stević,[2] Ratomir Jelić,[3] Sanja Matić,[3] Suzana Popović,[4] Predrag Djurdjević,[5,6] Dejan Baskić[4,7] and Biljana Petrović*[1]

[1]University of Kragujevac, Faculty of Science, Radoja Domanovića 12, 34000 Kragujevac, Serbia

[2]University of Kragujevac, Institute of Information Technologies, Jovana Cvijića bb, 34000 Kragujevac, Serbia

[3]University of Kragujevac, Faculty of Medical Sciences, Department of Pharmacy, Svetozara Markovića 69, 34000 Kragujevac, Serbia

[4]University of Kragujevac, Faculty of Medical Sciences, Centre for Molecular Medicine and Stem Cell Research, Svetozara Markovića 69, 34000 Kragujevac, Serbia

[5]University of Kragujevac, Faculty of Medical Sciences, Department of Internal medicine, Svetozara Markovića 69, 34000 Kragujevac, Serbia

[6]Clinic for Haematology, Clinical Centre Kragujevac, Zmaj Jovina 30, 34000 Kragujevac, Serbia

[7]Public Health Institute, Nikole Pašića 1, 34000 Kragujevac, Serbia

*Corresponding author: Prof. Dr. Biljana Petrović, Phone: +381(0)34336223,

Fax: +381(0)34335040, e-mail: biljana.petrovic@pmf.kg.ac.rs

Table S1. Clonogenic surival of HTB140 and H460 cells after **PP2** treatment.

	HTB140					
Conc. (µM)	0 (control)	1 µM	3 µM	10 µM	30 µM	100 µM
CA						
SF (mean)		**0.51**	**0.10**	**0.0025**	**0**	**0**
	H460					
Conc. (µM)	0 (control)	1 µM	3 µM	10 µM	30 µM	100 µM
CA						
SF (mean)		**0.025**	**0.0025**	**0**	**0**	**0**

Table S2. Observed *pseudo*-first order rate constants as a function of nucleophile concentration and temperature for the substitution reactions of **PP1** in 25 mM Hepes buffer (pH = 7.2), 50 mM NaCl.

Ligand	T [K]	λ [nm]	$10^3 C_L$ [M]	k_{obsd1} [s^{-1}]	k_{obsd2} [s^{-1}]
Tu	288	300	1	20.89(5)	10.49(4)
			2	39.73(3)	19.84(5)
			3	59.74(5)	30.74(4)
			4	79.26(4)	40.36(4)
			5	101.35(4)	50.94(5)
	298		1	28.23(3)	12.61(4)
			2	58.13(5)	24.19(4)
			3	87.03(4)	36.24(3)
			4	114.51(4)	48.87(5)
			5	143.89(3)	61.24(4)
	310		1	41.52(5)	16.47(4)
			2	80.17(4)	33.61(3)
			3	119.87(4)	50.13(4)
			4	160.23(3)	67.03(4)
			5	203.12(3)	83.24(3)

Ligand	T [K]	λ [nm]	$10^3 C_L$ [M]	k_{obsd1} [s^{-1}]	k_{obsd2} [s^{-1}]
L-Met	288	260	1	8.40(5)	3.59(5)
			2	15.98(4)	7.33(4)
			3	24.87(4)	11.05(5)
			4	33.01(3)	14.53(4)
			5	40.94(5)	18.21(3)
	298		1	9.73(4)	4.48(3)
			2	20.55(4)	8.88(5)
			3	30.13(3)	13.08(4)
			4	40.75(3)	17.65(4)
			5	50.02(5)	22.11(3)
	310		1	14.77(4)	6.43(5)
			2	29.97(5)	12.77(5)

Ligand	T [K]	λ [nm]	$10^3 C_L$ [M]	k_{obsd1} [s^{-1}]	k_{obsd2} [s^{-1}]
			3	46.15(4)	19.27(4)
			4	60.34(4)	25.37(5)
			5	74.88(4)	32.01(4)
GSH	288	260	1	5.29(4)	2.23(5)
			2	10.41(4)	4.39(4)
			3	15.37(3)	6.67(5)
			4	20.87(5)	8.84(5)
			5	25.97(4)	11.07(4)
	298		1	7.43(4)	3.21(5)
			2	15.11(3)	6.36(4)
			3	22.31(5)	9.45(4)
			4	29.75(4)	12.71(4)
			5	37.39(5)	15.85(3)
	310		1	10.51(4)	4.33(5)
			2	21.13(3)	8.57(4)
			3	31.18(5)	13.01(4)
			4	41.57(4)	17.13(3)
			5	52.53(4)	21.55(4)
Ligand	T [K]	λ [nm]	$10^3 C_L$ [M]	k_{obsd1} [s^{-1}]	k_{obsd2} [s^{-1}]
5'-GMP	288	320	1	3.23(5)	0.61(4)
			2	6.29(4)	1.27(3)
			3	9.41(5)	1.93(5)
			4	12.54(4)	2.51(4)
			5	15.83(3)	3.13(3)
	298		1	4.64(4)	0.88(5)
			2	9.01(3)	1.84(4)
			3	13.57(5)	2.73(4)
			4	18.03(4)	3.57(3)
			5	22.77(5)	4.46(5)
	310		1	6.25(4)	1.24(4)
			2	12.57(5)	2.55(4)

3	18.92(4)	3.77(5)
4	25.23(5)	4.97(4)
5	31.23(4)	6.21(3)

[a]Number of runs in parenthesis

Table S3. Observed *pseudo*-first order rate constants as a function of nucleophile concentration and temperature for the substitution reactions of **PP2** in 25 mM Hepes buffer (pH = 7.2), 50 mM NaCl.

Ligand	T [K]	λ [nm]	$10^3 \, C_L$ [M]	$10^3 \, k_{obsd1}$ [s^{-1}]	$10^4 \, k_{obsd2}$ [s^{-1}]
Tu	298	320	1	4.52(2)	6.33(2)
			2	9.31(2)	13.11(3)
			3	13.53(3)	19.20(2)
			4	18.01(2)	25.64(2)
			5	22.65(2)	32.11(3)

Ligand	T [K]	λ [nm]	$10^3 \, C_L$ [M]	k_{obsd1} [s^{-1}]	k_{obsd2} [s^{-1}]
L-Met	298		1	1.96(2)	2.31(2)
			2	3.85(2)	4.75(3)
			3	5.84(3)	7.11(2)
			4	7.81(2)	9.42(3)
			5	9.58(3)	11.62(2)

Ligand	T [K]	λ [nm]	$10^3 \, C_L$ [M]	k_{obsd1} [s^{-1}]	k_{obsd2} [s^{-1}]
GSH	298		1	1.22(2)	1.67(2)
			2	2.47(2)	3.35(2)
			3	3.78(3)	5.01(2)
			4	5.05(2)	6.58(2)
			5	6.11(3)	8.27(3)

Ligand	T [K]	λ [nm]	$10^3 \, C_L$ [M]	k_{obsd1} [s^{-1}]	k_{obsd2} [s^{-1}]
5'-GMP	298		1	0.91(2)	1.15(2)
			2	1.78(3)	2.37(3)
			3	2.63(2)	3.45(2)
			4	3.56(2)	4.61(3)
			5	4.42(3)	5.71(2)

[a]Number of runs in parenthesis

Table S4. Observed *pseudo*-first order rate constants as a function of nucleophile concentration and temperature for the substitution reactions of **PP3** in 25 mM Hepes buffer (pH = 7.2), 50 mM NaCl.

Ligand	T [K]	λ [nm]	$10^3\,C_L$ [M]	k_{obsd1} [s^{-1}]	$10^3\,k_{obsd2}$ [s^{-1}]
Tu	298	290	1	15.88(5)	4.07(2)
			2	31.75(4)	8.36(2)
			3	47.09(5)	12.47(2)
			4	63.52(4)	16.47(2)
			5	78.94(3)	20.53(2)

Ligand	T [K]	λ [nm]	$10^3\,C_L$ [M]	k_{obsd1} [s^{-1}]	k_{obsd2} [s^{-1}]
L-Met	298	265	1	5.68(4)	1.58(2)
			2	10.53(4)	3.16(2)
			3	15.72(4)	4.68(2)
			4	21.55(5)	6.22(3)
			5	26.85(5)	7.83(2)

Ligand	T [K]	λ [nm]	$10^3\,C_L$ [M]	k_{obsd1} [s^{-1}]	k_{obsd2} [s^{-1}]
GSH	298	260	1	3.36(4)	0.79(5)
			2	6.83(3)	1.58(2)
			3	10.33(5)	2.37(2)
			4	13.63(4)	3.14(2)
			5	16.85(5)	3.96(3)

Ligand	T [K]	λ [nm]	$10^3\,C_L$ [M]	k_{obsd1} [s^{-1}]	k_{obsd2} [s^{-1}]
5'-GMP	298	320	1	1.27(3)	0.56(2)
			2	2.63(5)	1.14(3)
			3	4.01(4)	1.69(2)
			4	5.21(4)	2.23(2)
			5	6.47(5)	2.79(3)

[a]Number of runs in parenthesis
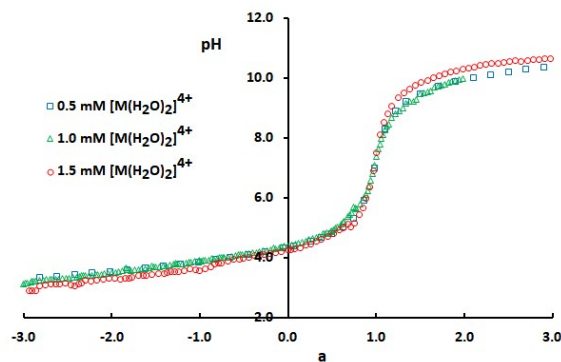
Figure S1. Potentiometric titration of $[M(H_2O)_2]^{4+}$ ion (M = $[Pd_2L]^{4+}$ and L = tpbd) with standard NaOH in 0.1 M $NaClO_4$ ionic medium at 298 K.
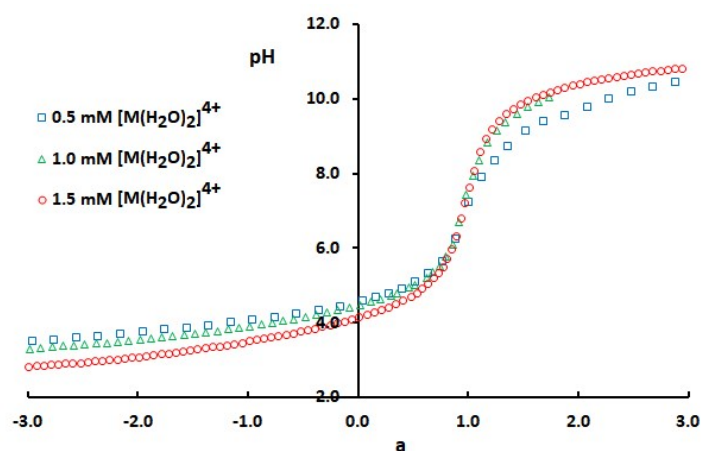
Figure S2. Potentiometric titration of $[M(H_2O)_2]^{4+}$ ion (M = $[Pt_2L]^{4+}$ and L = tpbd) with standard NaOH in 0.1 M $NaClO_4$ ionic medium at 298 K.
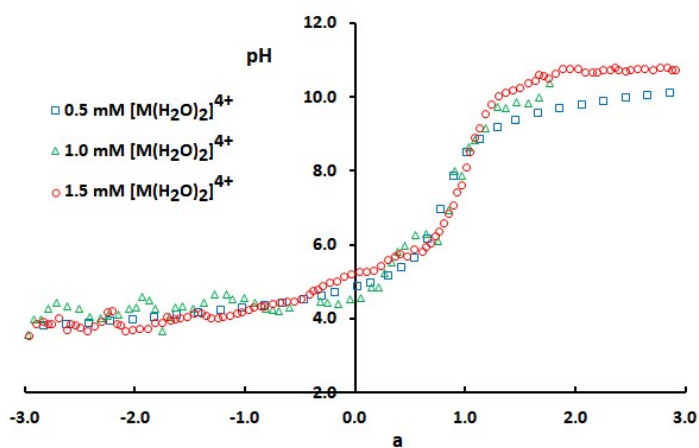
Figure S3. Potentiometric titration of $[M(H_2O)_2]^{4+}$ ion (M = $[PdPtL]^{4+}$ and L = tpbd) with standard NaOH in 0.1 M $NaClO_4$ ionic medium at 298 K.
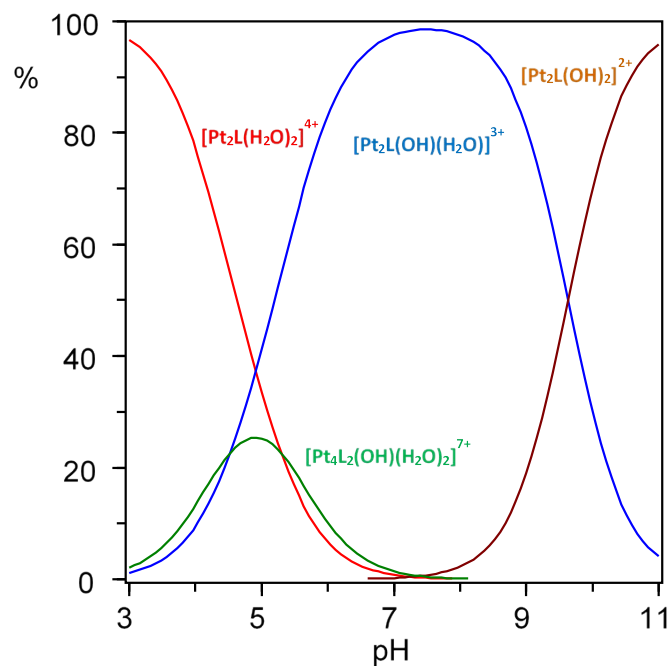
Figure S4. Distribution diagram of the species formed in 0.1 M NaClO$_4$ ionic medium at 298 K for [Pt$_2$L(H$_2$O)$_2$]$^{4+}$ (M), C$_M$ = 1 × 10^{-3}M.
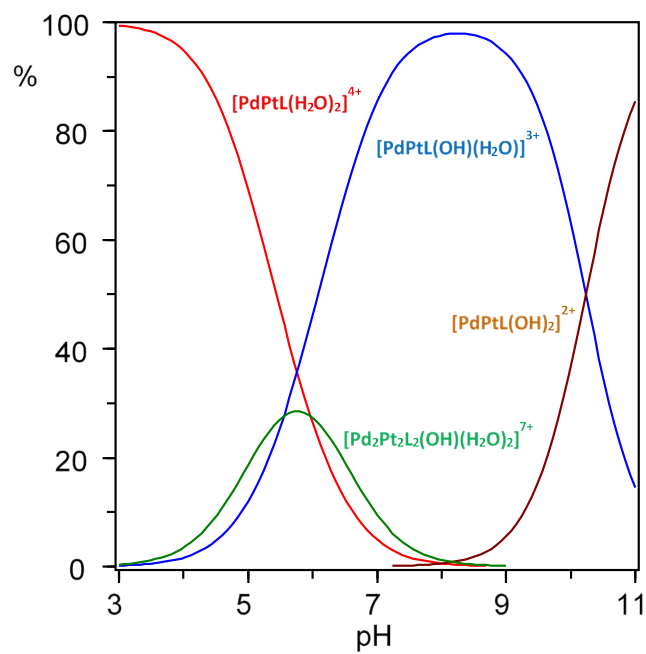
Figure S5. Distribution diagram of the species formed in 0.1 M NaClO$_4$ ionic medium at 298 K for [PdPtL(H$_2$O)$_2$]$^{4+}$ (M), C$_M$ = 1 × 10^{-3}M.
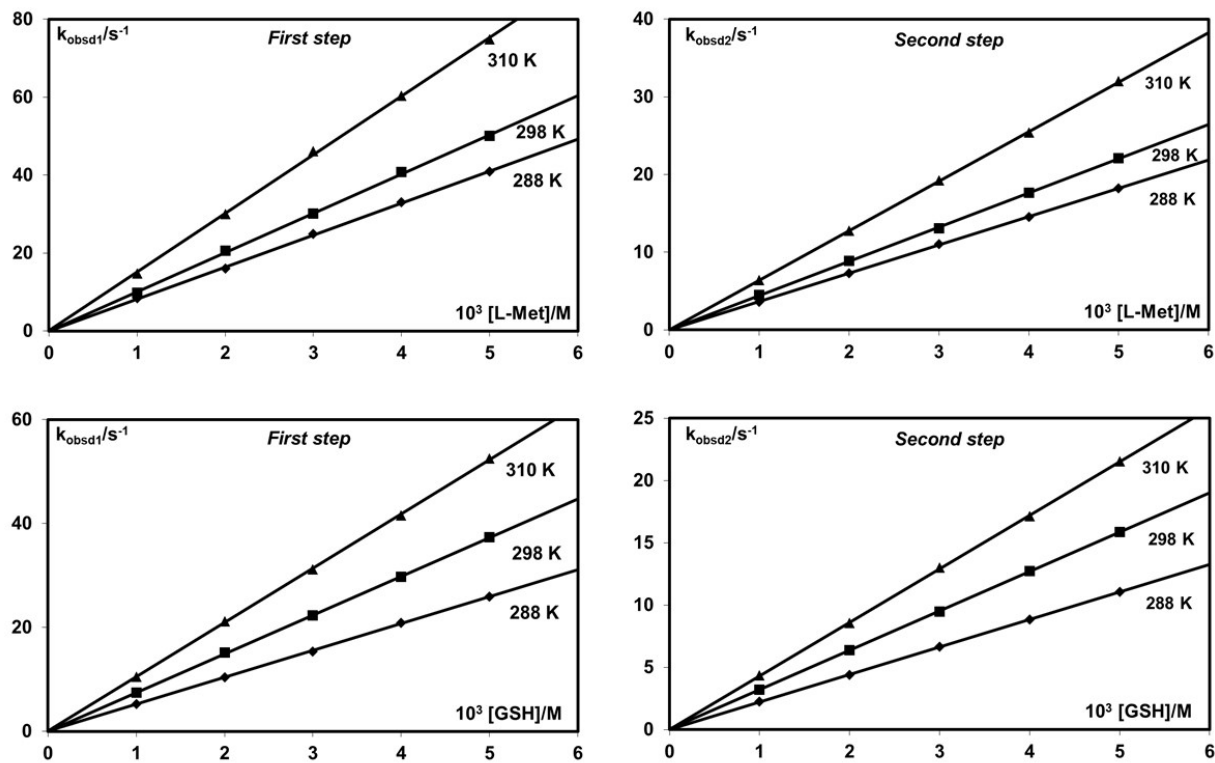
Figure S5. Plots of the $k_{obsd(i)}$ *vs*. nucleophile concentration at three different temperatures for the substitution reactions of **PP1** with L-Met and GSH, $I = 25$ mM Hepes buffer, 50 mM NaCl.
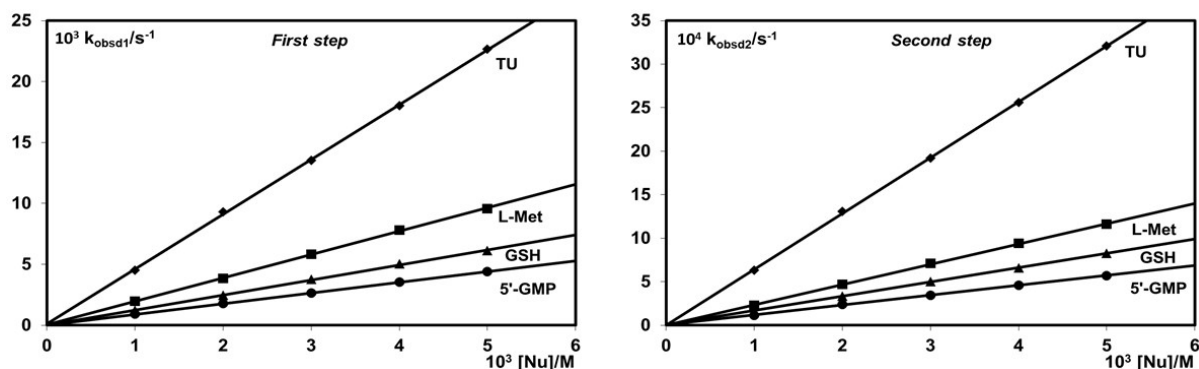
Figure S7. Plots of $k_{obsd(i)}$ *vs.* nucleophile concentration at 298 K for the substitution reaction of **PP2**, I = 25 mM Hepes buffer, 50 mM NaCl.
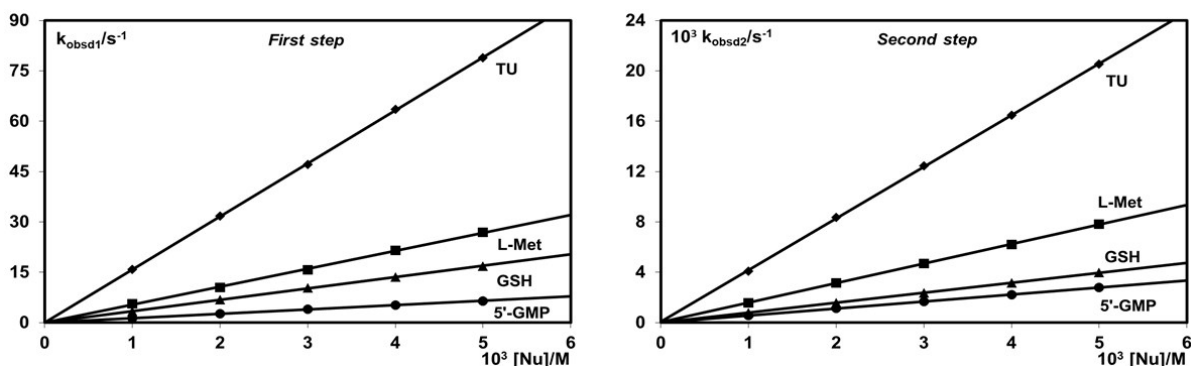
Figure S8. Plots of $k_{obsd(i)}$ *vs.* nucleophile concentration at 298 K for the substitution reaction of **PP3**, I = 25 mM Hepes buffer , 50 mM NaCl.
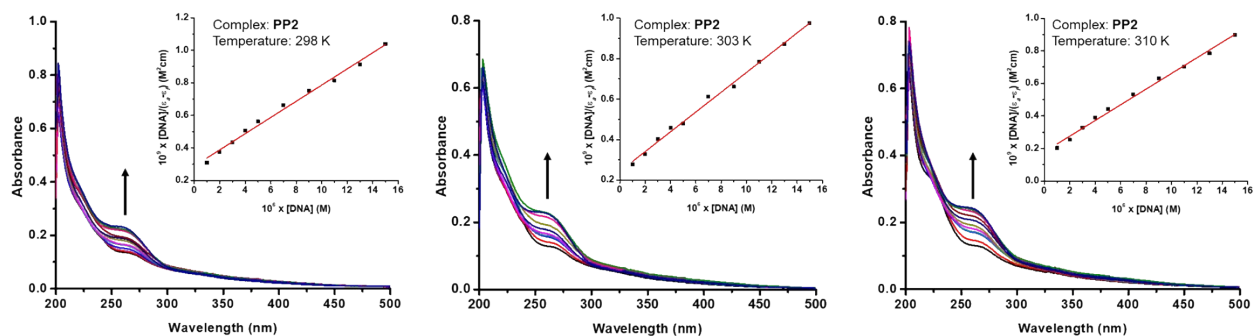
Figure S9. Absorption spectra of **PP2** at different temperatures in PBS buffer upon addition of CT-DNA. [complex]= 1×10^{-5} M, [DNA]= $(0–1.5) \times 10^{-5}$ M. Arrow shows the change of absorbance with the increase of DNA concentrations. Inset: plot of $[DNA]/(\varepsilon_a - \varepsilon_f)$ vs. [DNA].
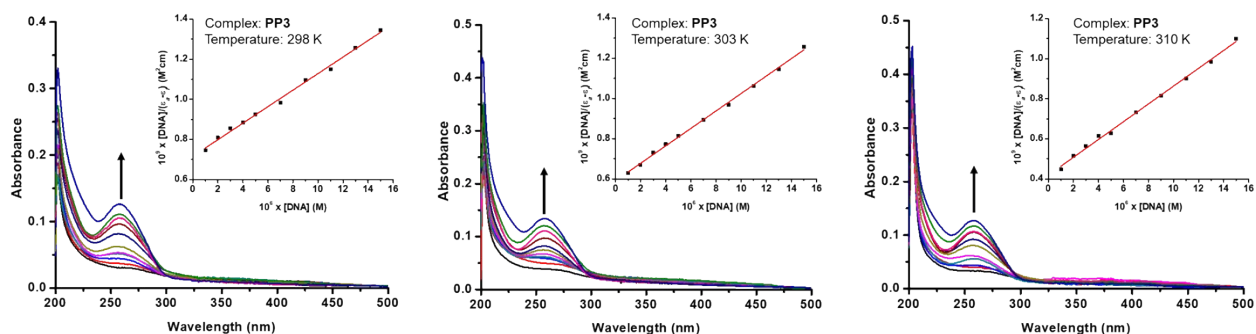
Figure S10. Absorption spectra of **PP3** at different temperatures in PBS buffer upon addition of CT-DNA. [complex]= 1×10^{-5} M, [DNA]= $(0–1.5) \times 10^{-5}$ M. Arrow shows the change of absorbance with the increase of DNA concentrations. Inset: plot of [DNA]/$(\varepsilon_a - \varepsilon_f)$ vs. [DNA].
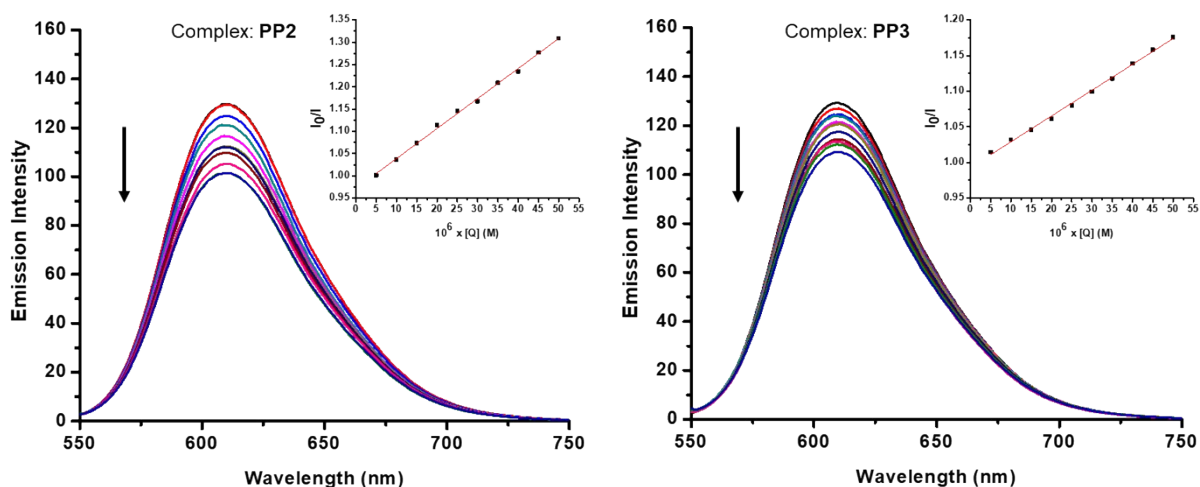
Figure S11. Emission spectra of EB bound to DNA in the presence of **PP2** and **PP3**. [EB]= 25 μM; [DNA]= 25 μM; [complex]= (0-50) μM; λ_{ex}=527 nm. Arrows show the intensity changes upon increasing the concentration of complex. Inset graph: Plot of I_0/I *vs.* [Q], with ■ for the experimental data points and the full line for the linear fitting of the data.
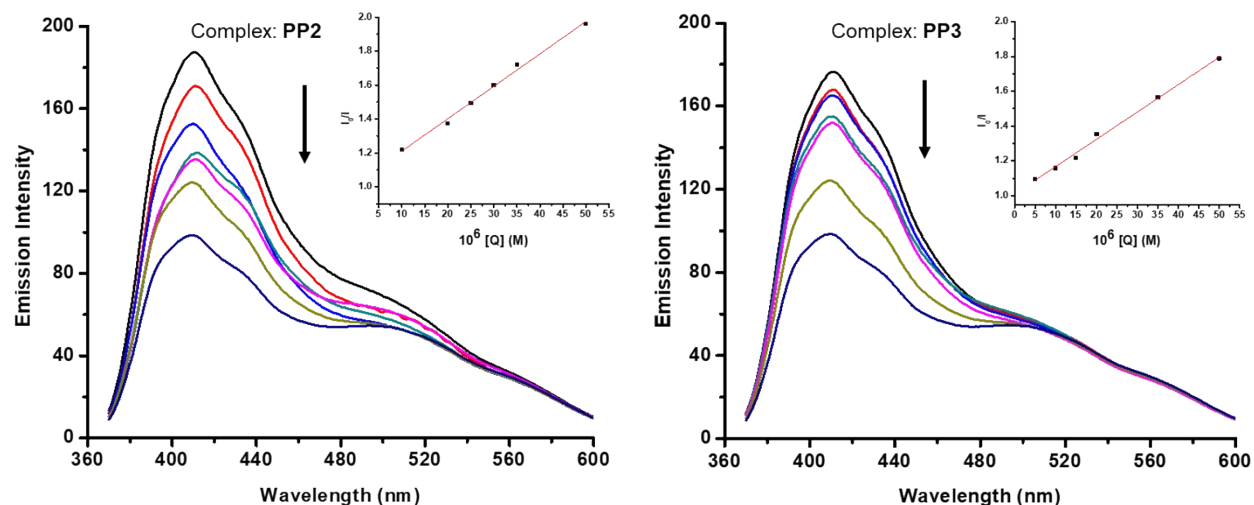
Figure S12. Emission spectra of Hoe bound to DNA in the presence of **PP2** and **PP3**. [Hoe] = 25 µM; [DNA] = 25 µM; [complex]= (0 - 50) µM; λ_{ex} = 346 nm. Arrows show the intensity changes upon increasing the concentration of complex. Inset graph: Plot of I_0/I *vs.* [Q], with ■ for the experimental data points and the full line for the linear fitting of the data.
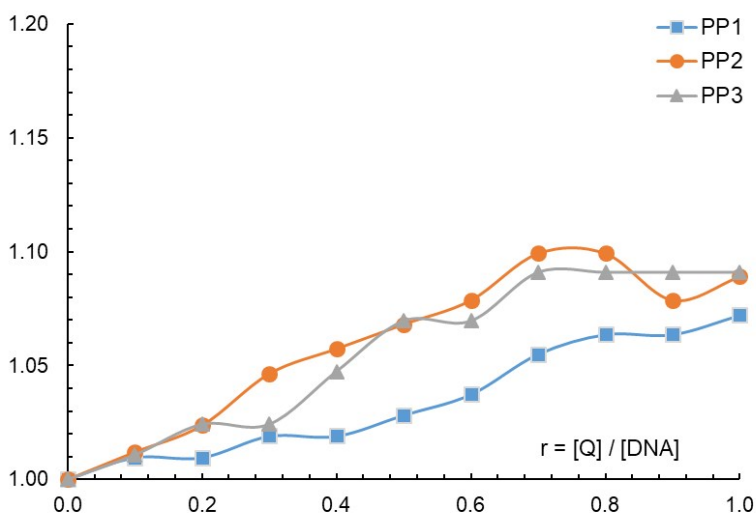
Figure S13. Relative viscosity $(\eta/\eta_0)^{1/3}$ of CT-DNA (0.01 mM) in PBS buffer solution with the addition of increasing amounts (r) of **PP1**, **PP2** and **PP3** complexes.
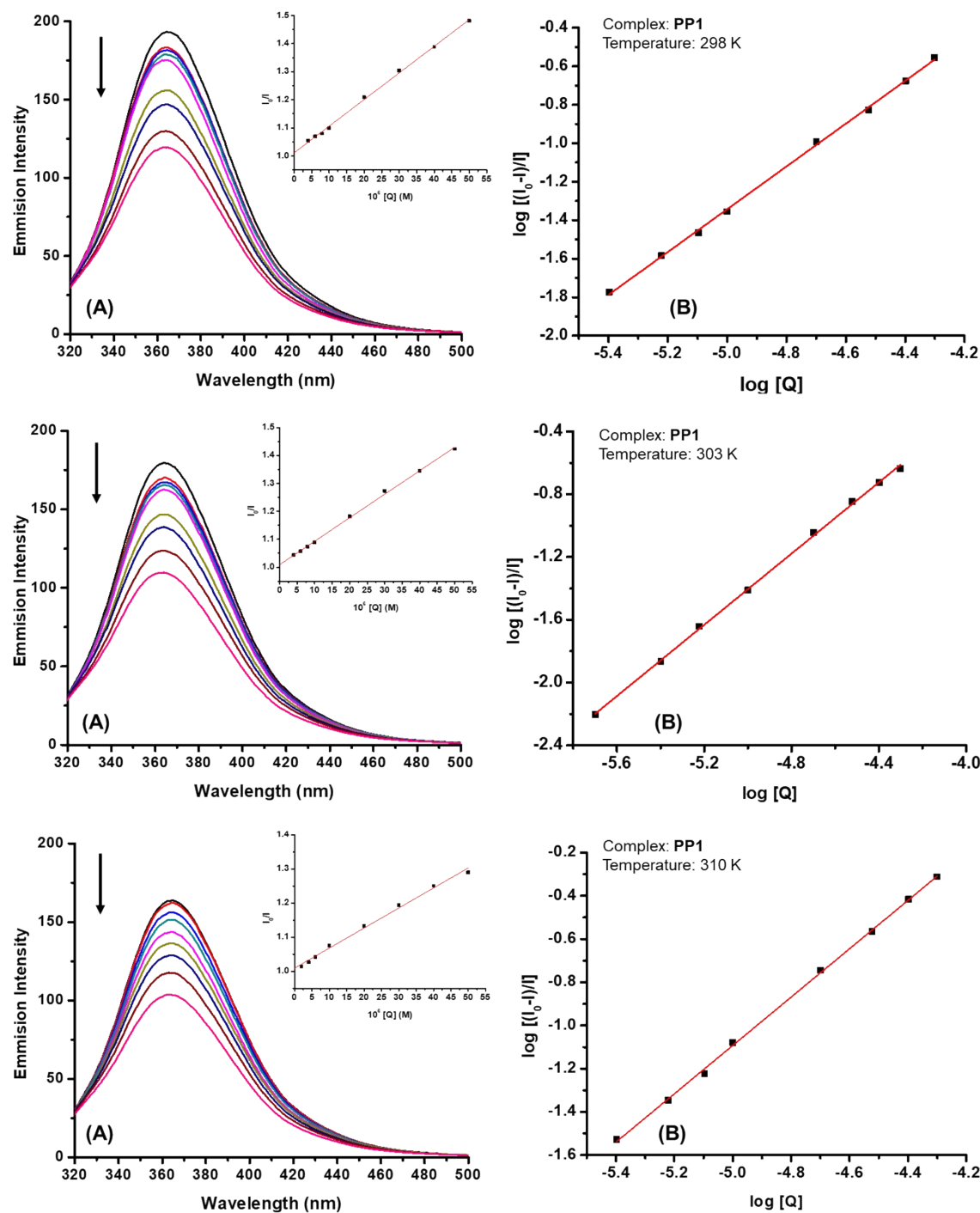
Figure S14. (A) Emission spectra of BSA in the presence of **PP1** at different temperatures. [BSA] = 2 μM, [complex] = 0 – 50 μM, λ_{ex} = 285 nm. Arrows show the intensity changes upon increasing the concentrations of complex. Inset graph: Plot of I_0/I *vs.* [Q], with ■ for the experimental data points and the full line for the linear fitting of the data; (B) Plot of $\log[(I_0-I)/I]$ *vs.* $\log[Q]$ for BSA-PP1 complex system at different temperatures.
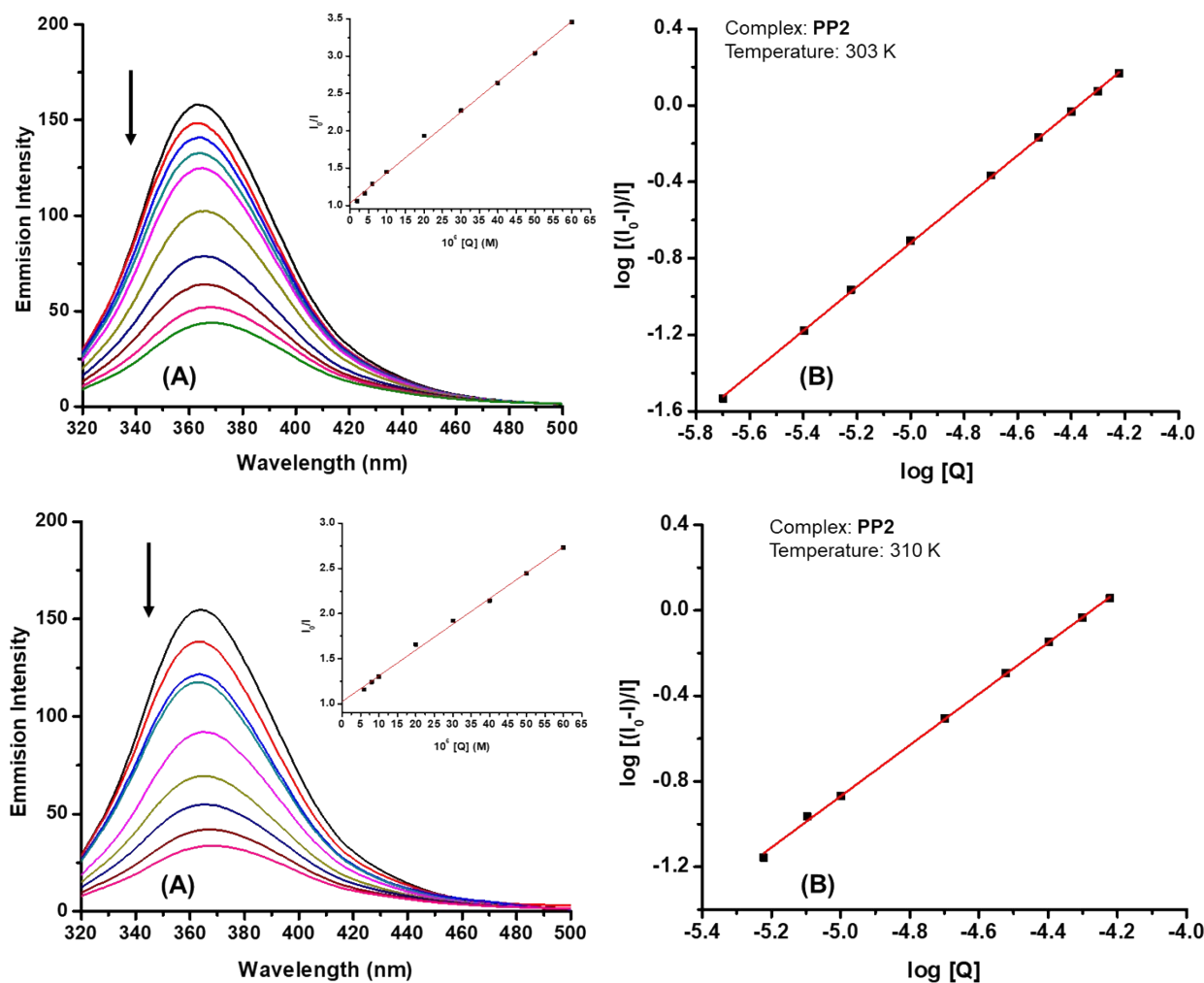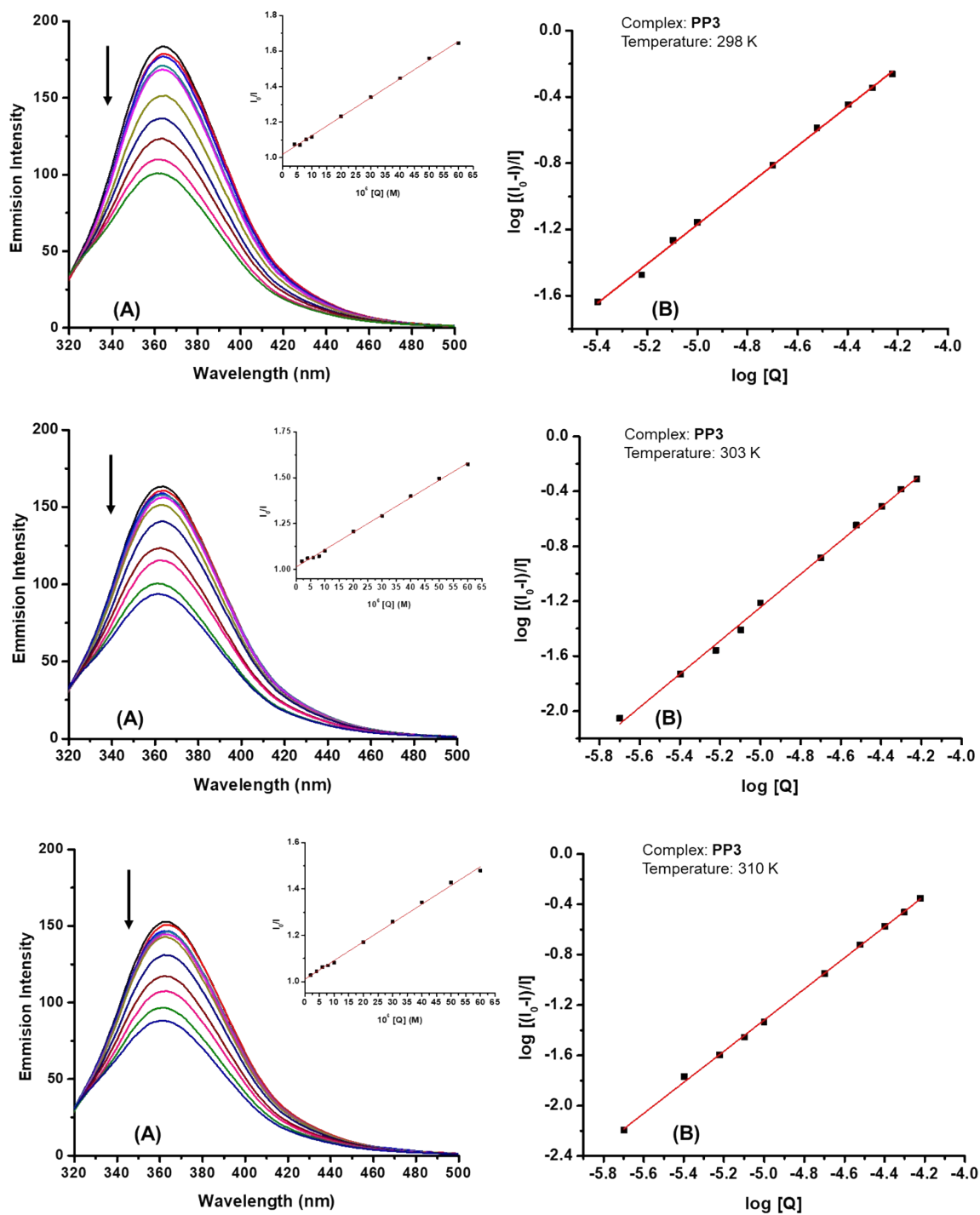
Figure S15. (A) Emission spectra of BSA in the presence of **PP2** at different temperatures. [BSA] = 2 μM, [complex] = 0 – 60 μM, λ_{ex} = 285 nm. Arrows show the intensity changes upon increasing the concentrations of complex. Inset graph: Plot of I_0/I *vs.* [Q], with ■ for the experimental data points and the full line for the linear fitting of the data; (B) Plot of $\log[(I_0-I)/I]$ *vs.* $\log[Q]$ for BSA-PP2 complex system at different temperatures.

Figure S16. (A) Emission spectra of BSA in the presence of **PP3** at different temperatures. [BSA] = 2 μM, [complex] = 0 – 60 μM, λ_{ex} = 285 nm. Arrows show the intensity changes upon increasing the concentrations of complex. Inset graph: Plot of I_0/I *vs.* [Q], with ■ for the experimental data points and the full line for the linear fitting of the data; (B) Plot of $\log[(I_0-I)/I]$ *vs.* $\log[Q]$ for BSA-PP3 complex system at different temperatures.

S6
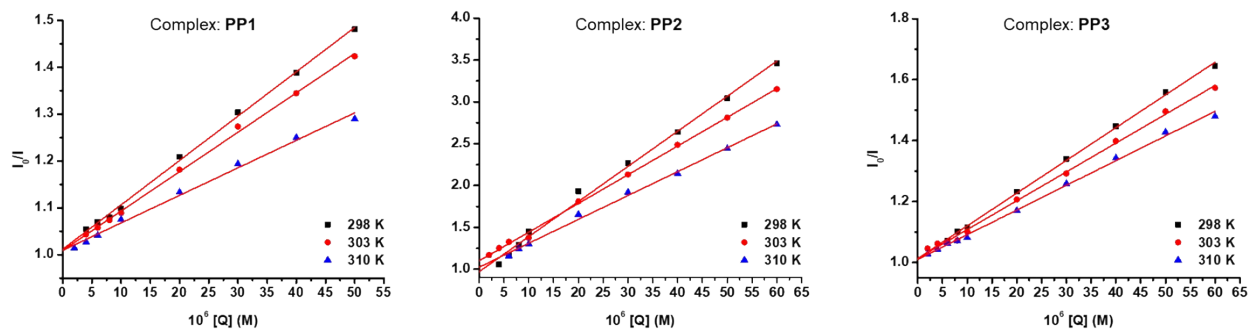
Figure S17. Stern-Volmer plots describing BSA quenching caused by **PP1**, **PP2** and **PP3** complexes at three different temperatures.
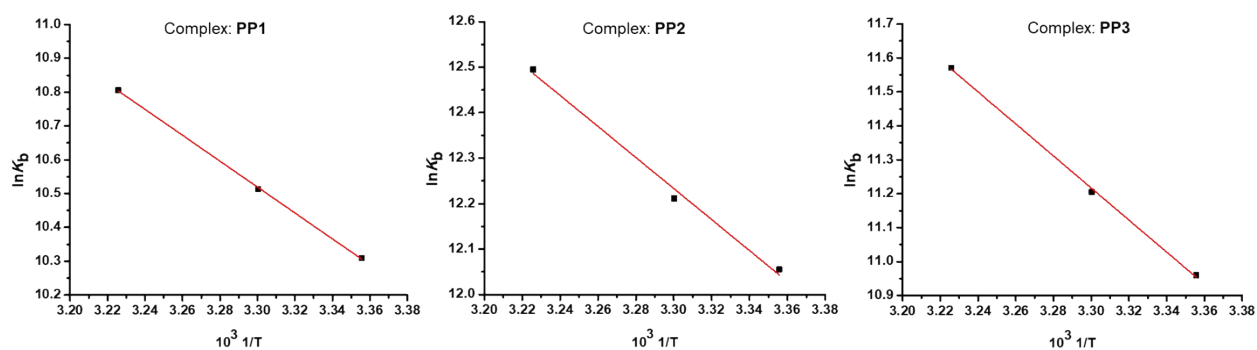

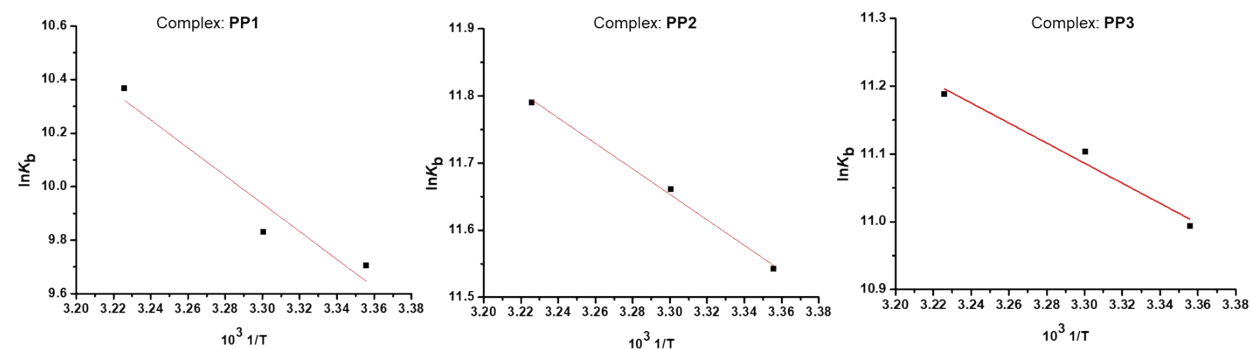**Figure S18.** Vant't Hoff plots for the binding of CT-DNA to investigated complexes.

Figure S19. Vant't Hoff plots for the binding of BSA to investigated complexes.
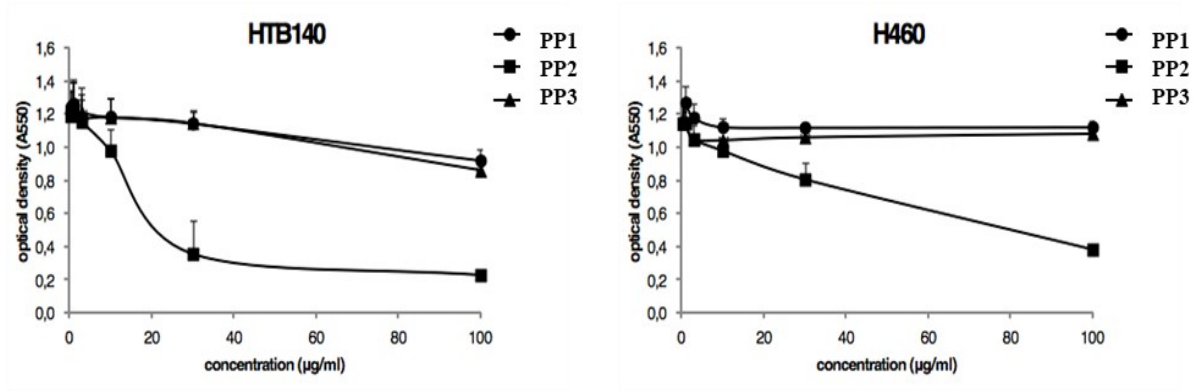
Figure S20. Dose-response curves of HTB14 and H460 cells treated for 48 h with six concentrations of **PP1**, **PP2** and **PP3** determined by MTT assay.
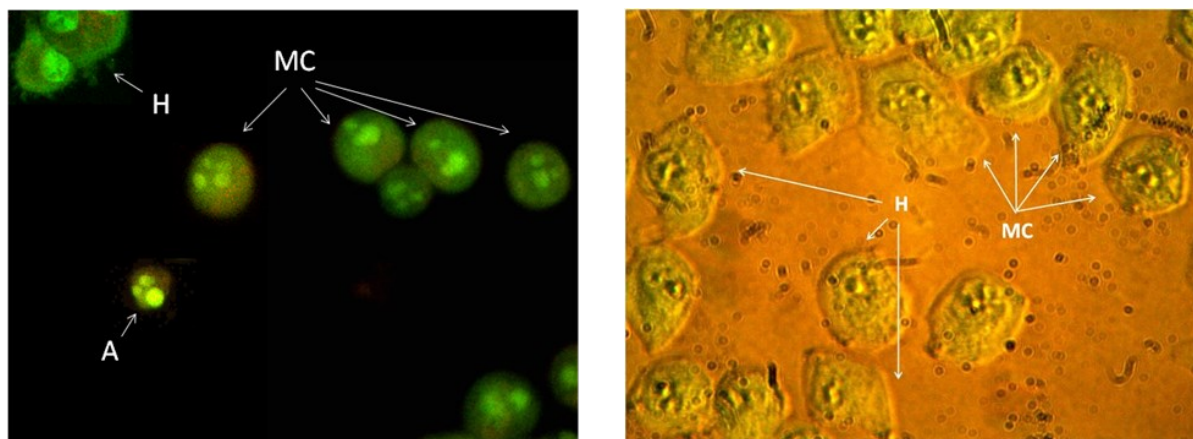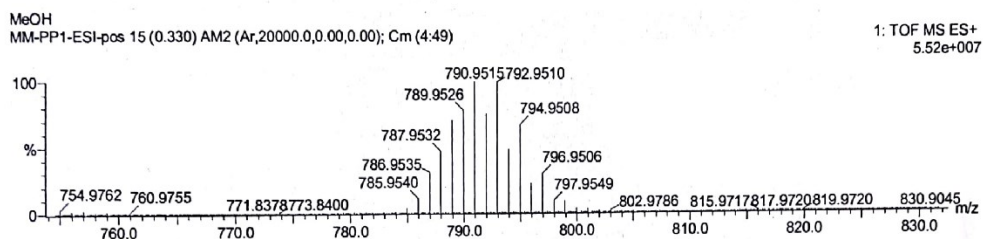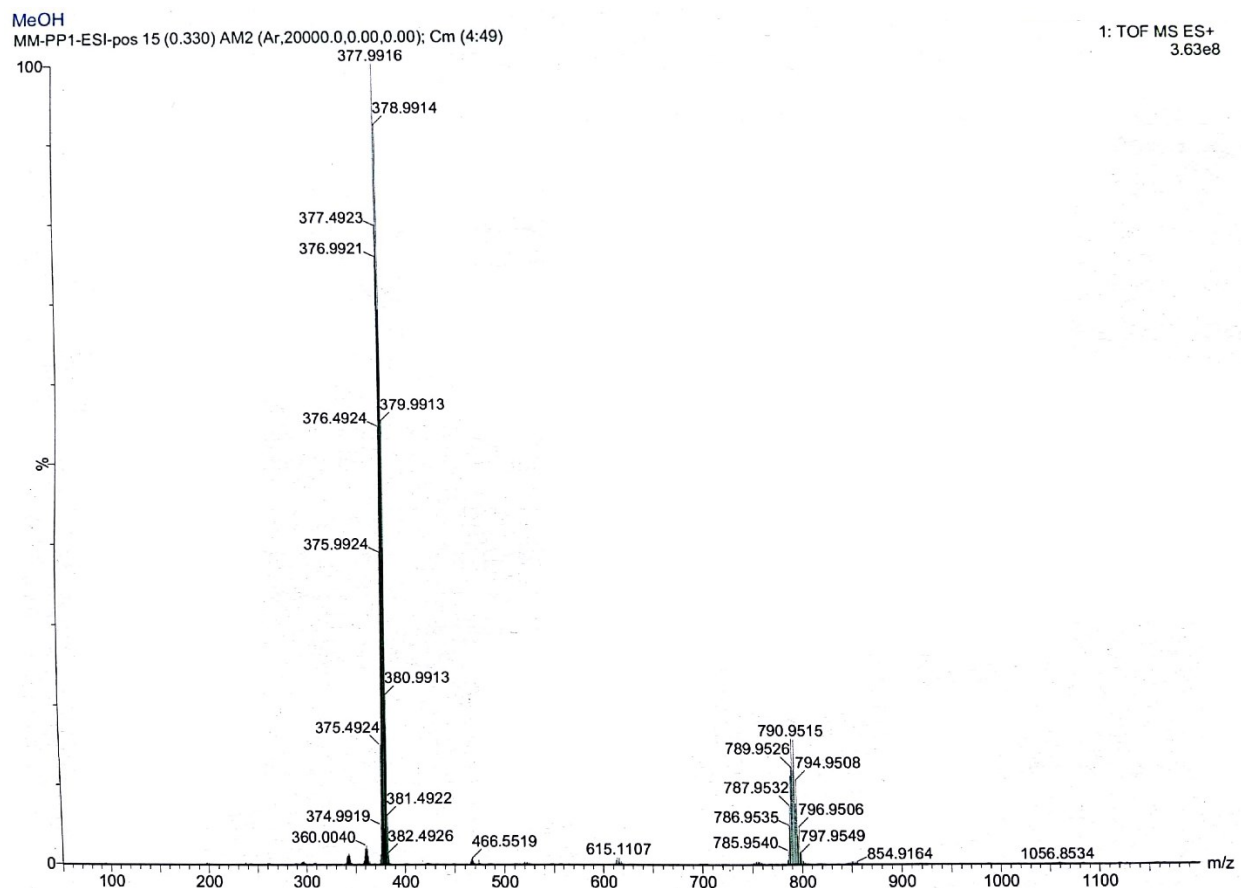

Figure S21. Mitotic catastrophe following treatment with **PP2**; Fluorescence microscopy of AO/EB stained cells (left panel) showing: apoptotic cells (A) characterized by cell shrinkage, nuclear fragmentation and condensation that results in homogeneous bright green fluorescence; multinucleated cells undergoing mitotic catastrophe (MC) with organized structure of uncondensed chromatin; healthy cells (H) with nucleus with organized structure. Right panel is representative image obtained by inverted microscope.

1: TOF MS ES+
3.63e8

100−

377.9916

378.9914

377.4923

376.9921

%−

376.4924

379.9913

375.9924

380.9913

375.4924

790.9515
789.9526
794.9508
787.9532
796.9506
381.4922
786.9535
374.9919
382.4926
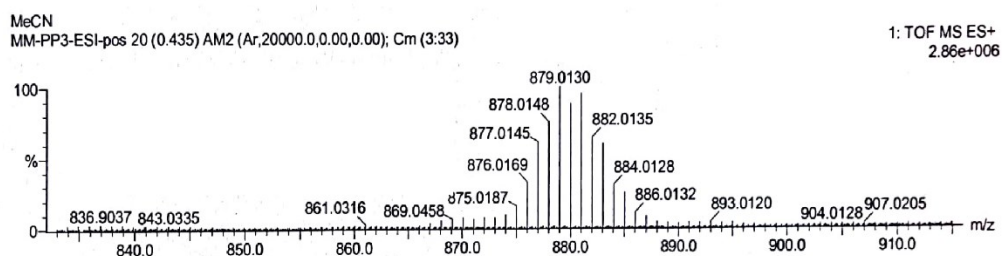360.0040
466.5519
615.1107
785.9540
797.9549
854.9164
1056.8534

0−

m/z
100   200   300   400   500   600   700   800   900   1000   1100

MeOH
MM-PP1-ESI-pos 15 (0.330) AM2 (Ar,20000.0,0.00,0.00); Cm (4:49)

1: TOF MS ES+
5.52e+007

100−

790.9515 792.9510

789.9526

794.9508

%−

787.9532

786.9535
785.9540

796.9506

797.9549

754.9762 760.9755

771.8378 773.8400

802.9786 815.9717 817.9720 819.9720

830.9045

0−

m/z
760.0   770.0   780.0   790.0   800.0   810.0   820.0   830.0

			Minimum:		−1.5			
			Maximum:	5.0	10.0	50.0		
Mass	Calc. Mass	mDa	PPM	DBE	i-FIT	Norm	Conf(%)	Formula
788.9518	788.9511	0.7	0.9	18.5	340.8	n/a	n/a	C30 H28 N6 Cl3 Pd2

Figure S22. ESI-MS spectrum of PP1 complex.

MM-PP2-ESI-pos 13 (0.296) AM2 (Ar,20000.0,0.00,0.00); Cm (4:51)

1: TOF MS ES+
9.50e7

100

448.0631

448.5636

467.0523

447.5622

467.5527

447.0597

468.0526

%

703.1711
702.1718

468.5529

430.0739

701.1693

704.1716

429.0689

469.0532

428.5655

473.2455

706.1749

876.0189

969.0720

1102.0223

495.2282

971.0721

289.1458

613.1133

873.0146 879.0233

1104.0225

0

80.0502

168.9183 286.5684

660.0699

m/z

100   200   300   400   500   600   700   800   900   1000   1100

MeCN
MM-PP2-ESI-pos 13 (0.296) AM2 (Ar,20000.0,0.00,0.00); Cm (4:51)

1: TOF MS ES+
5.58e+006

100

969.0720

967.0720   970.0721

966.0721   971.0721

%

972.0727

965.0701

974.0725

935.0958

947.0499 949.0519

964.0695

983.0529 985.0530   995.0736   1003.0334

0

m/z

940.0   950.0   960.0   970.0   980.0   990.0   1000.0

Minimum:				-1.5			
Maximum:		5.0	10.0	50.0			
Mass	Calc. Mass	mDa	PPM	DBE	i-FIT	Norm	Conf(%)	Formula
967.0720	967.0737	-1.7	-1.8	20.5	239.7	n/a	n/a	C30 H28 N6 Cl3 Pt2

Figure S23. ESI-MS spectrum of PP2 complex.

MM-PP3-ESI-pos 20 (0.435) AM2 (Ar,20000.0,0.00,0.00); Cm (3:33)

1: TOF MS ES+
3.71e7

MeCN
MM-PP3-ESI-pos 20 (0.435) AM2 (Ar,20000.0,0.00,0.00); Cm (3:33)

1: TOF MS ES+
2.86e+006
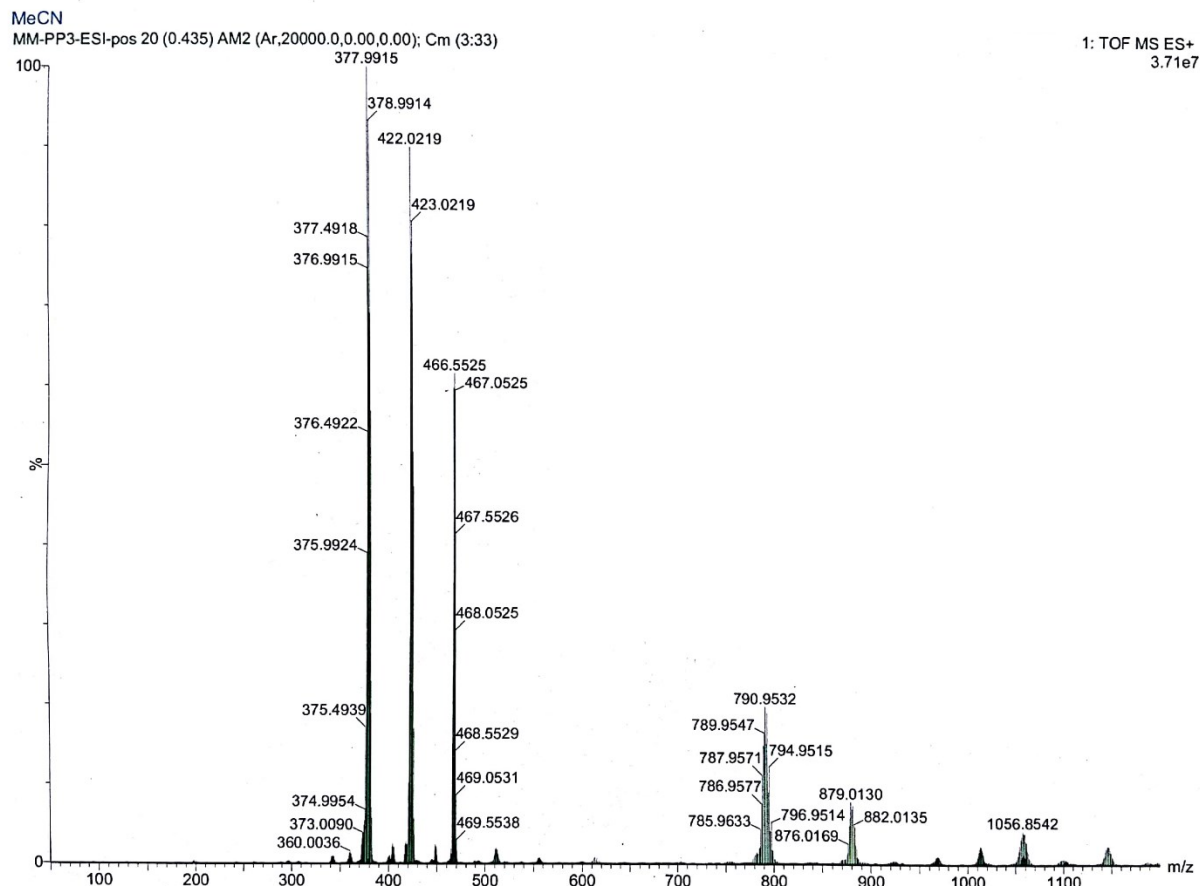
			Minimum:			-1.5				
Maximum:				5.0	10.0	50.0				
Mass	Calc. Mass	mDa	PPM	DBE	i-FIT	Norm	Conf(%)	Formula		
878.0148	878.0124	2.4	2.7	19.5	328.3	n/a	n/a	C30 H28 N6 Cl3 Pd Pt		

Figure S24. ESI-MS spectrum of PP3 complex.
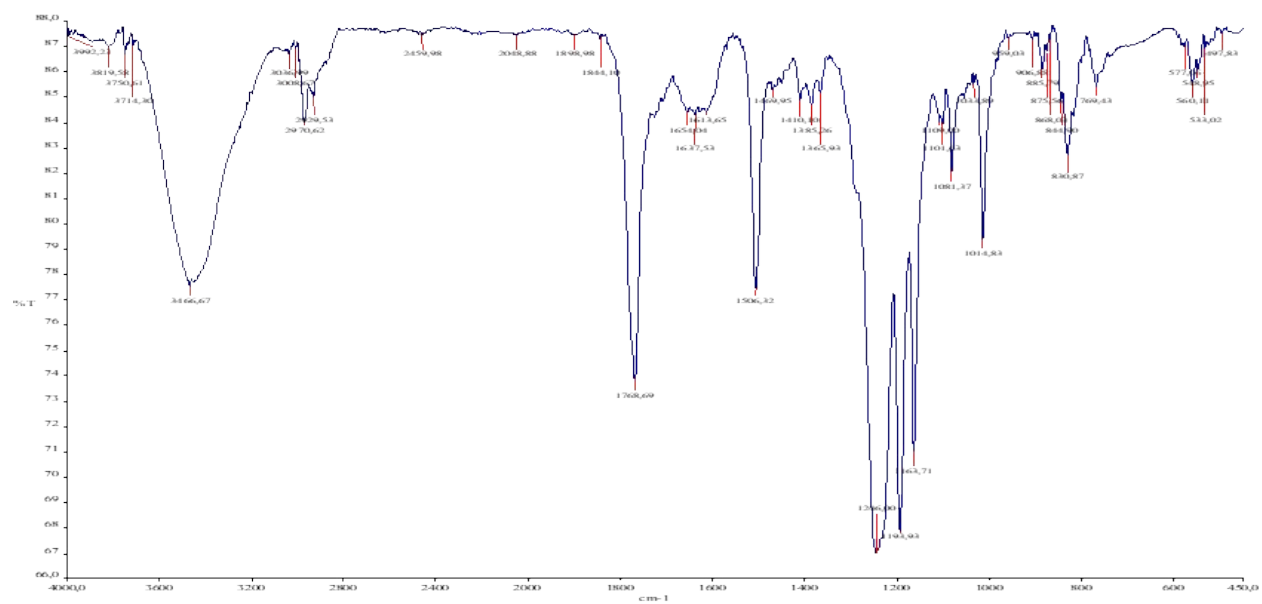
Figure S25. IR spectrum of PP1 complex.
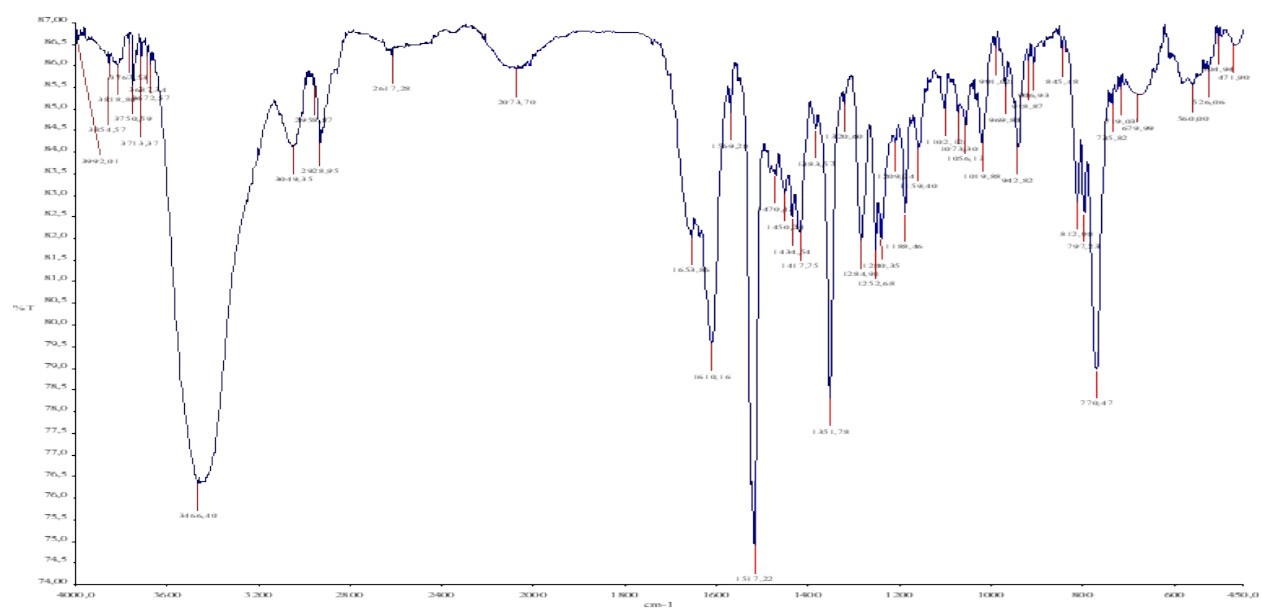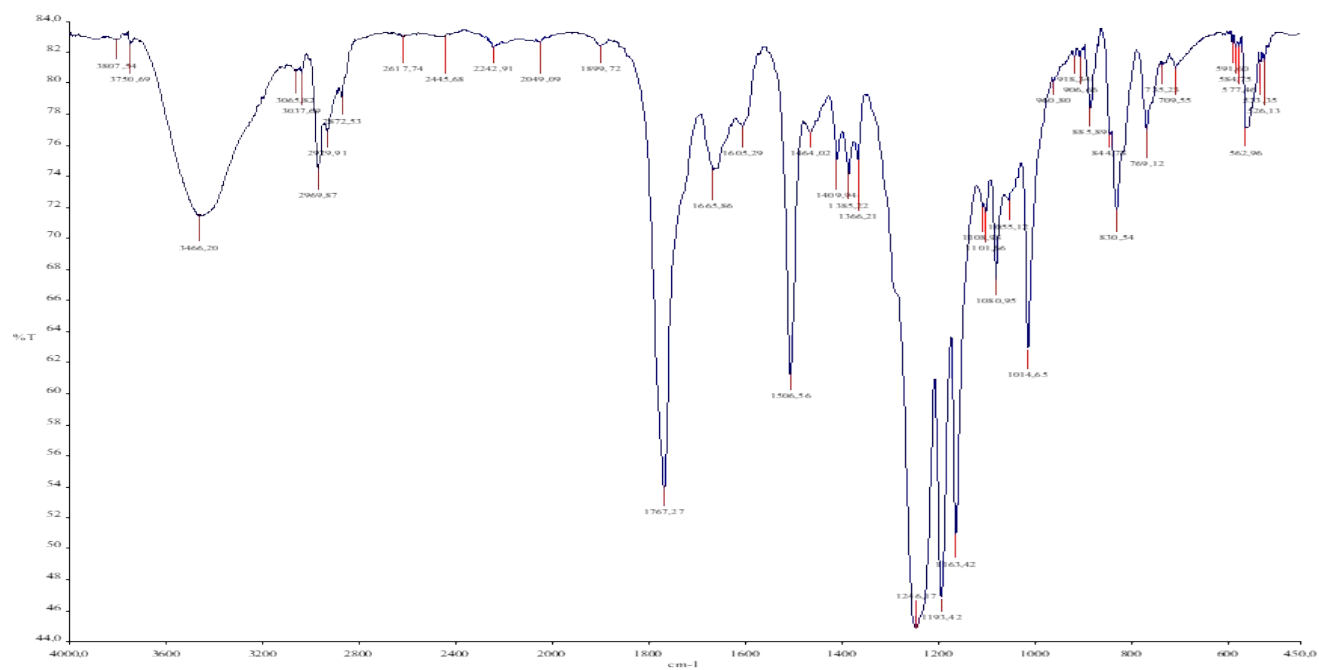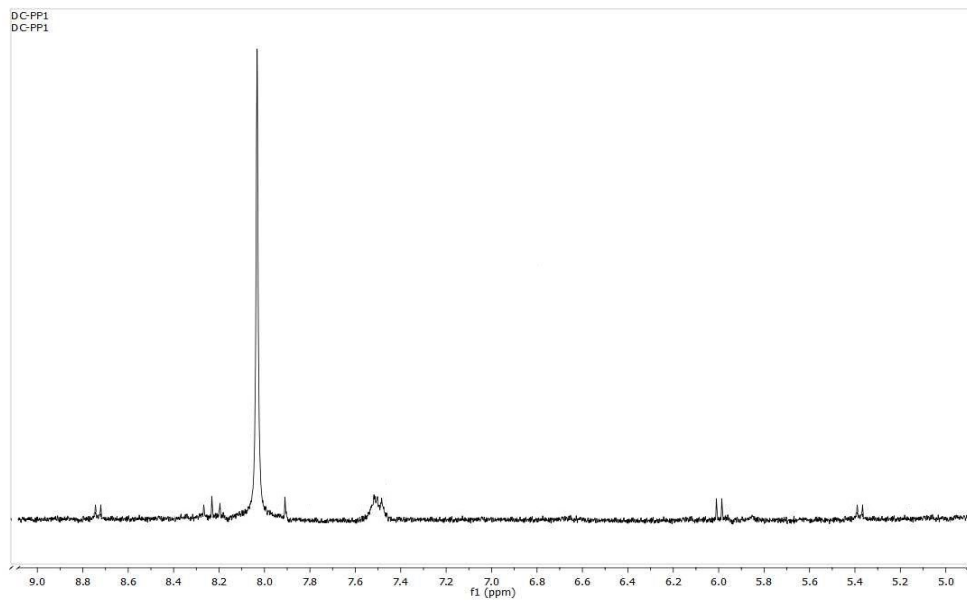

Figure S26. IR spectrum of PP2 complex.

Figure S27. IR spectrum of PP3 complex.
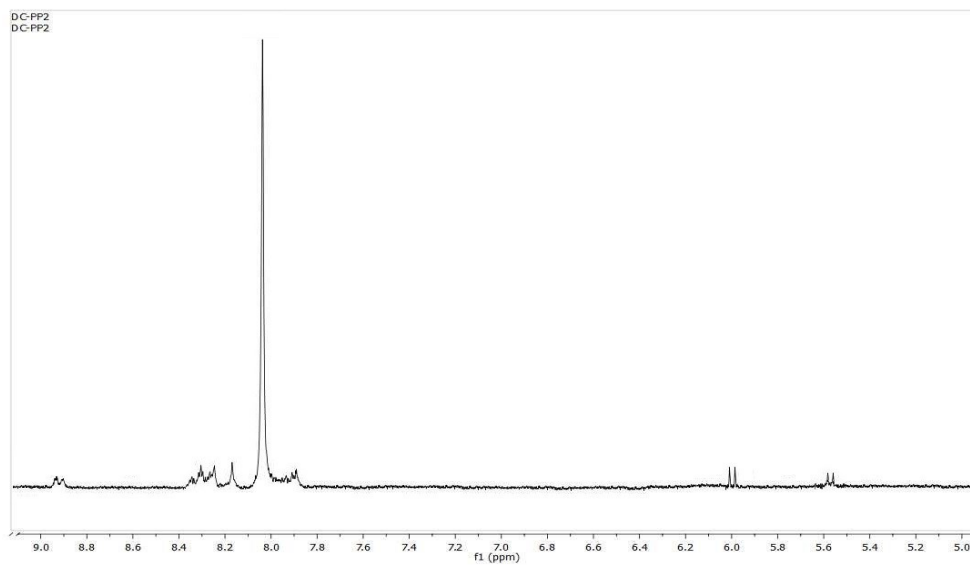
Figure S28. ^{1}H NMR spectrum of PP1 complex.

Figure S29. ^{1}H NMR spectrum of PP2 complex.

DC-PP3
DC-PP3

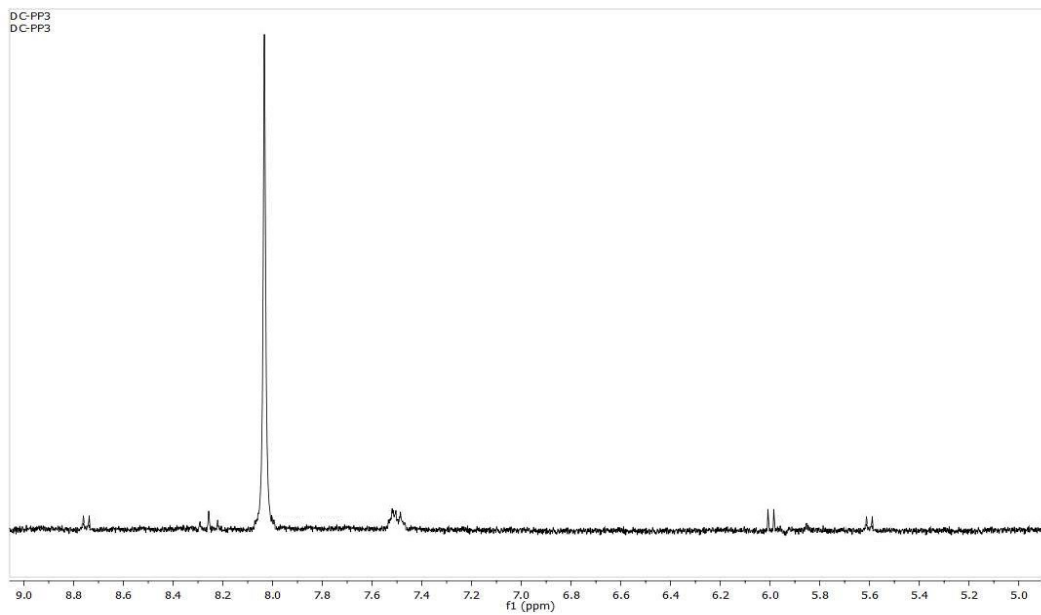9.0 8.8 8.6 8.4 8.2 8.0 7.8 7.6 7.4 7.2 7.0 6.8 6.6 6.4 6.2 6.0 5.8 5.6 5.4 5.2 5.0
f1 (ppm)

Figure S30. ^{1}H NMR spectrum of PP3 complex.